

## GEOMAGNETIC EFFECTS OF SLOPING AND SHELVING DISCONTINUITIES OF EARTH CONDUCTIVITY†

F. WALTER JONES\* AND ALBERT T. PRICE‡

The surface effects on electric and magnetic variations arising from interfaces in three two-dimensional conductivity models are compared in detail for four frequencies. It is found that the horizontal extent of the surface effects greatly depends on the dimensions of the different structures relative to the skin depths at the frequencies used. Also, a fundamentally important difference

is revealed between *H*-polarization and *E*-polarization problems in that the apparent resistivity computed on the surface near the contact is discontinuous and changes abruptly in the *H*-polarization case, whereas for *E*-polarization the apparent resistivity is continuous and changes gradually across the contact.

### INTRODUCTION

In recent work by Jones and Price (1969, 1970a), we considered the perturbation of an alternating geomagnetic field by an abrupt vertical discontinuity in conductivity and determined in detail the magnetic field and current distributions throughout the composite conductor. The technique applied was that of solving the equations and boundary conditions by means of the Gauss-Seidel iteration method. Our model was two-dimensional with a vertical contact between the two regions of different conductivity (model 1 in Figure 1). Two polarization cases (*H*-polarization, where the magnetic field is parallel to the strike, and *E*-polarization, where the electric field is parallel to the strike) were solved. We have now extended our technique to consider two more models and have made comparisons of the surface effects of the discontinuities for the different models.

### THE MODELS

The coordinate system and the three models are shown in Figure 1.

Model 1 is the original model (Jones and Price, 1970a), which consists of a semi-infinite conduct-

ing region composed of two quarter-spaces of different conductivity.

Model 2 is one with a sloping contact between the two regions of the conductor. The slope is 45 degrees and, rather than being continuous, is actually stepped, since the numerical method involves the solution of equations and boundary conditions over a uniform square grid. Model 2 is therefore termed the "step" model.

Model 3 is called the "shelf" model. In it, a shelf-type contact exists between the two regions of different conductivity in the conducting half-space.

In all three models, the grid spacing is taken as 1.5 km. The mesh is square and contains 1681 grid points (41 × 41), modeling, therefore, a cross-section 60 km square. The surface of the earth is taken as the center horizontal row of grid points, and the surface contact between the two conducting regions is the center point of this line. For model 2, the steps are one grid spacing in height (1.5 km) and one grid spacing in width (1.5 km). In model 3, the depth from the surface to the shelf is 4 grid spacings (6.0 km) and the length of the shelf is 11 grid spacings (16.5 km).

These models have some of the features of an

† Received by the Editor June 16, 1970; revised manuscript received October 19, 1970.

\* Department of Physics, University of Alberta, Edmonton, Alberta, Canada.

‡ Department of Mathematics, University of Exeter, Exeter, England.

© 1971 by the Society of Exploration Geophysicists. All rights reserved.

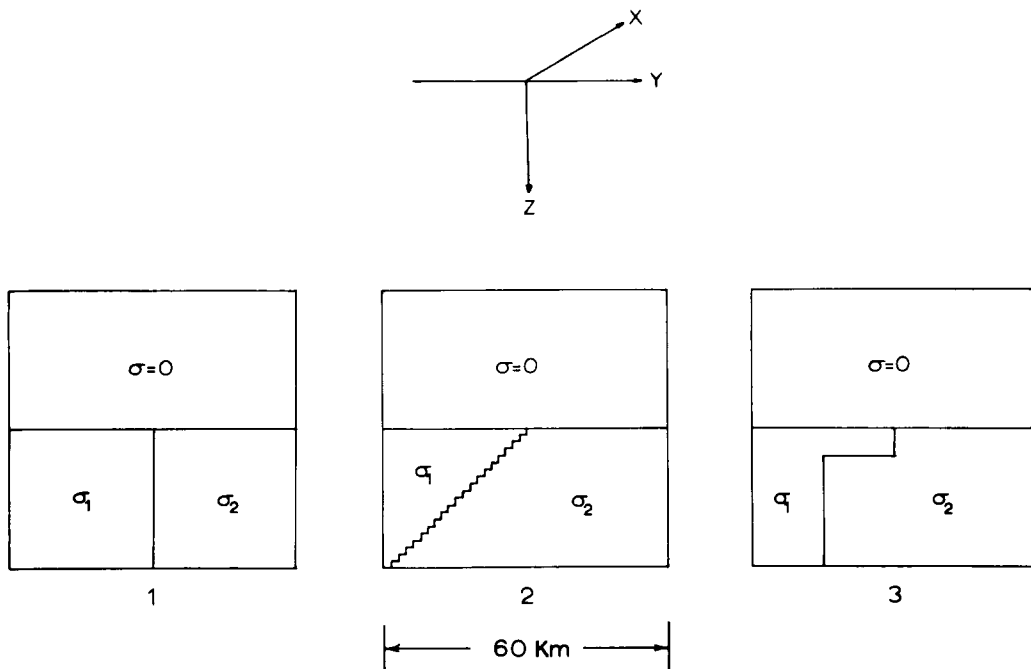


FIG. 1. The coordinate system and the three models used: (1) the vertical contact model, (2) the step model, (3) the shelf model.

Downloaded 01/27/16 to 171.66.208.139. Redistribution subject to SEG license or copyright; see Terms of Use at http://library.seg.org/

ocean-continental boundary, but neither model 2 nor model 3 accurately approximates an actual continental shelf, since the ocean depth over the actual shelf is much less and the width of the shelf is much greater than those of the models. Since a square grid is used, we cannot obtain a depth-to-width ratio which represents correctly the true continental shelf. However, by considering the models used, we can gain some understanding of the various effects and can apply what we learn to the actual situation.

The conductivities chosen were  $\sigma_1 = 4.0$  mho-m<sup>-1</sup> (resistivity = 0.25 ohm-m) and  $\sigma_2 = 10^{-3}$  mho-m<sup>-1</sup> (resistivity = 1000 ohm-m). These are approximate conductivities for sea water and the continental crust. The frequencies investigated were 0.01 hz (100 sec period), 0.003 hz (approximately 5.6 minute period), 0.001 hz (approximately 16.7 minute period), and 0.0003 hz (approximately 55.6 minute period). The skin depths for the two conductivities at these frequencies are given in Table 1.

**NUMERICAL FORMULATION OF THE PROBLEM**

The equations to be solved in all regions for both cases have the form

$$\nabla^2 F = i\eta^2 F, \quad (\text{Jones and Price 1970a}),$$

with the appropriate value of  $\eta$  (a function of the conductivity) inserted;  $F$  represents either  $H_x$  or  $E_x$ .

If  $F = f + ig$ ,  $\nabla^2 F = \nabla^2(f + ig) = \nabla^2 f + i\nabla^2 g$  and  $i\eta^2 F = i\eta^2(f + ig) = i\eta^2 f - \eta^2 g$ . Equating real and imaginary parts, we obtain  $\nabla^2 f = -\eta^2 g$  and  $\nabla^2 g = \eta^2 f$ .

These two equations are replaced by corresponding finite difference equations, which are then solved simultaneously for each point on the mesh by finite difference methods. The methods also take into account the boundary conditions (Jones and Price 1970a).

**THE SURFACE EFFECTS**

We shall consider the three models in detail by comparing the surface values of the fields and the components which may be calculated for the  $H$ -polarization and  $E$ -polarization cases. Also the phases of the components and various ratios are considered.

*H-polarization*

For  $H$ -polarization,  $H_x$  is constant along the surface (Jones and Price 1970a). Also, for both

Table 1. Skin depths of the conductors for the four frequencies used

	0.01 hz	0.003 hz	0.001 hz	0.0003 hz
$\sigma_1 = 4.0 \text{ mho-m}^{-1}$	2.52 km	4.59 km	7.96 km	14.53 km
$\sigma_2 = 10^{-3} \text{ mho-m}^{-1}$	159.2 km	290.6 km	503.3 km	918.8 km

$H$ -polarization and  $E$ -polarization,  $E_x$  along the surface is zero (Jones and Price, 1970a). Therefore, the only component calculated is  $E_y$ , the horizontal component of the electric field. Since  $H_x$  is constant, we may also find  $E_y/H_x$ ; and  $\rho_A$ , the apparent resistivity, may be calculated for this polarization. The phase of the horizontal component of the electric field ( $\phi_{E_y}$ ) is computed along the surface. The phase of  $E_y$  is calculated relative to the phase at the end point over the region of lower conductivity.

In Figure 2, the amplitude of  $E_y$ , the phase of  $E_y$  ( $\phi_{E_y}$ ), and  $\rho_A$  are plotted along the surface for the 3 models for the 4 frequencies considered in Table 1.

From Figure 2, we can see that  $E_y$  is discontinuous over the abrupt change of conductivity at the surface. Since  $H_x$  is constant along the surface for this polarization,  $E_y/H_x$  is of the same form as  $E_y$ ; and  $\rho_A$  is also discontinuous at the contact as shown.

A remarkable feature of the diagrams for  $\rho_A$  is that this "apparent resistivity" sharply decreases (i.e. the apparent conductivity *increases*) as the interface is approached from the more highly conducting ("seaward") side, and that  $\rho_A$  increases (though less remarkably) as the interface is approached from the "landward" side. Also, for the longer period variations,  $\rho_A$  is smaller (i.e., the apparent conductivity is *higher*) in the area where the shelf is present. Moreover,  $\rho_A$  is higher for the slower variations than for the faster ones. This behavior would imply, according to the usual magnetotelluric interpretation, an increase of conductivity with depth in the neighborhood of the shelf, whereas in models 2 and 3 there is actually a sudden decrease in the real conductivity. The explanation of this curious feature is that, in the case of  $H$ -polarization, the currents are flowing parallel to the cross-sections shown in Figure 1 and impinge against the interface, where a surface charge is built up. The amount of current needed to build up this surface charge is negligibly small, but the electric field of this charge is quite important. It acts so as to

reduce  $E_y$  in the high conductivity region and so as to increase  $E_y$  in the low conductivity region. Consequently, the *apparent* resistivity, inferred from the resultant  $E_y$  at the surface by use of the Cagniard formula, is reduced near the interface in the highly conducting region and increased in the low conductivity region. This buildup of surface charge on the interface is encountered in all  $H$ -polarization problems (Jones and Price, 1970a). Most of the surface effects on the field components are due to surface charge buildup and consequently these field components cannot be used directly in the usual magnetotelluric formula to infer the actual conductivity distribution.

For the frequency 0.01 hz,  $E_y$  for models 1 and 3 is nearly the same. Since the skin depth in the higher conducting region is considerably less than the depth from the surface to the shelf of model 3, the effect of the shelf is not seen at the surface. However, the value of  $E_y$  for model 2 dips down near the contact. In this case, the skin depth of the higher conducting region is greater than the depth of one step and nearly equal to the depth of two steps. Therefore, the effects of the first two steps appear at the surface. A similar situation is seen for  $\phi_{E_y}$  and  $\rho_A$  for this frequency; although the shelf (model 3) does slightly affect the phase.

For the frequency 0.003 hz, the skin depth in  $\sigma_1$  is approximately equal to 3 step depths and the effect of these steps is demonstrated by the variation of the components further from the contact in model 2. Also, the skin depth is now beginning to approach the depth of the shelf of model 3, so that its presence is detected in  $E_y$  and  $\rho_A$  and is strongly shown in  $\phi_{E_y}$ .

For 0.001 hz, the skin depth is greater than 5 step heights of model 2; thus the influence of the subsurface structure is being felt even further from the surface contact. The skin depth is now greater than the depth to the shelf of model 3 and the presence of the shelf is clearly indicated. It may also be seen that there is some change in the calculated functions for model 1 throughout the 4 frequencies. The cutoff appears to become less abrupt for the longer periods in this model, but, as already stated, the surface effects are, in the main, due to charge accumulated on the boundary.

For 0.0003 hz, the subsurface structure is even more evident. The skin depth in the higher con-

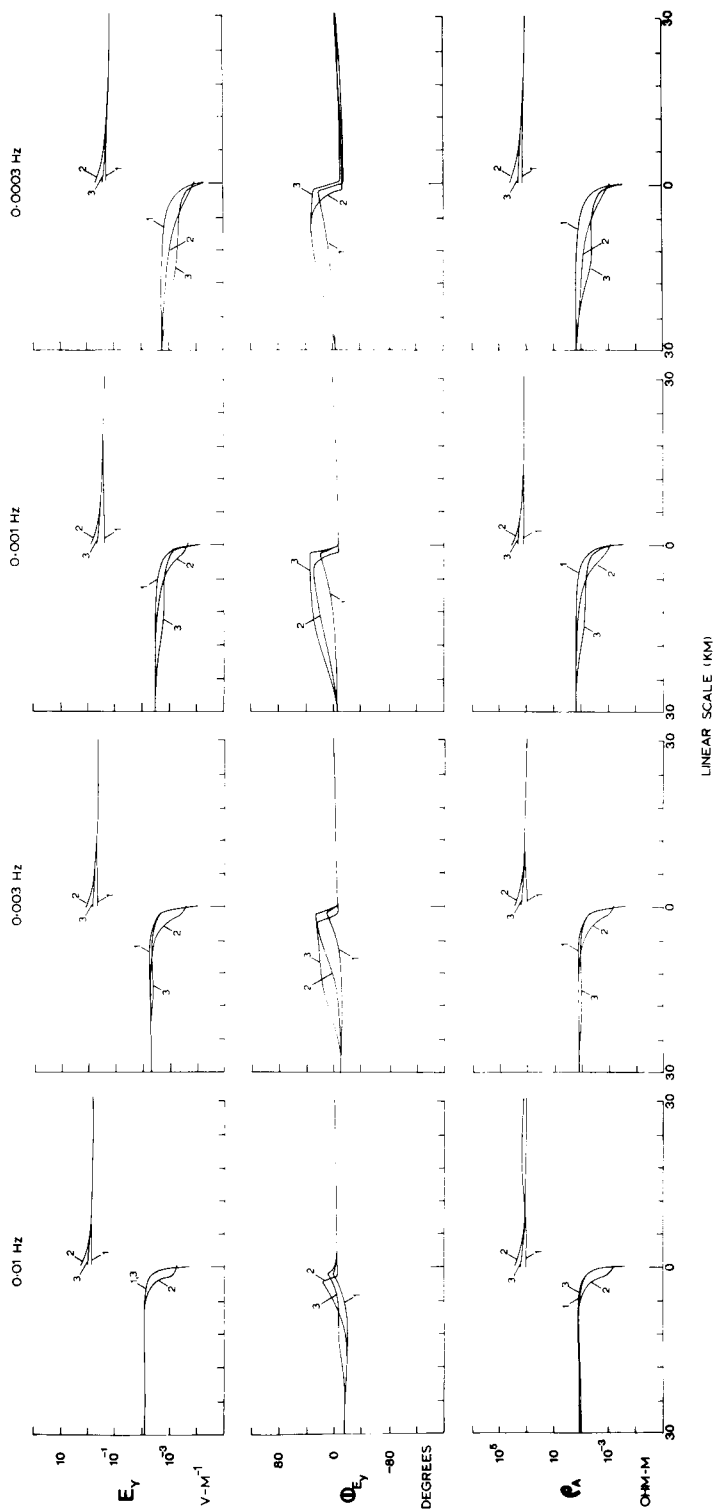


FIG. 2.  $H$ -polarization.  $E_y$ ,  $\phi_{E_y}$ , and  $\rho_A$  for the (1) vertical, (2) step, and (3) shelf models.

ducting region is 14.53 km at this frequency; consequently, about 10 steps will appreciably influence the surface effects of model 2. However, since the steps go deeper as the distance from the contact increases, the effect is different from that in model 3, where the depth to the shelf is fixed. It is seen that, at a distance from the surface contact,  $\phi_{E_y}$  for the shelf and step models is the same but differs near the contact.

### *E-polarization*

In the solution for the *E*-polarization, the amplitudes of  $E_x$ ,  $H_y$ , and  $H_z$  are calculated, as well as their phases relative to the end point. Also, the ratios  $E_x/H_y$  and  $H_z/H_y$  and the apparent resistivity  $\rho_A$  are computed.

Figure 3 shows  $E_x$ ,  $H_y$ , and  $H_z$  for the 3 models for the 4 frequencies considered. All 3 components are continuous across the discontinuity for this polarization (Jones and Price 1970b). For all 3 components, the surface contact of the discontinuity is most obvious for the highest frequency and becomes less prominent as the period increases. Also, we observe that  $H_y$  and  $H_z$  increase as the period increases.

For  $E_x$ , the effect of the step and shelf become apparent at 0.003 hz, and the two models are indistinguishable at 0.0003 hz.

Figure 3 indicates that across the surface of the discontinuity the variation of  $H_y$  is considerably less than the variation of  $H_z$ . Also,  $H_z$  and  $H_y$  are of the same order of magnitude. This behavior may be compared with the previous result obtained from model 1, when a conductivity ratio of 10 to 1 was used (Jones and Price, 1970a). In the previous work, the values of  $H_y$  and  $H_z$  were of the same order of magnitude and the variation of  $H_y$  and  $H_z$  across the contact was nearly the same size. Also, a comparison may be made with a buried inhomogeneity (Jones and Price, 1970b), for which the conductivity ratio was 100 to 1. In making these comparisons, we must take into account the difference in frequencies, which are lower for our present work than in our previous studies.

Again in  $H_y$  and  $H_z$  the subsurface structure is evident at 0.003 hz, for which the skin depth in the higher conducting region is most nearly equal to the depth of the structures.

Figure 4 gives the ratios  $E_x/H_y$ ,  $H_z/H_y$ , and the apparent resistivity  $\rho_A$ . Once more the sub-

surface structure is most apparent at 0.003 hz, a frequency for which the skin depth is about equal to 3 steps in model 2 and approaches the depth of the shelf of model 3. At 0.01 hz, there is an apparent minimum in  $H_z/H_y$  over the corner of the shelf in model 3. This becomes a local maximum at the lower frequencies. The apparent resistivity curves show that at the higher conducting end of the models,  $\rho_A = 0.25$  ohm-m and at the lower conducting end,  $\rho_A = 1000$  ohm-m. These values give the correct conductivities for calculations for a uniform earth at a great distance from the contact. The increase in  $\rho_A$  is apparent over the subsurface structures near the surface contact as the frequencies decrease from 0.01 hz to 0.0003 hz and the influence of the lower conducting region below the shelves becomes stronger at longer periods. In the case of *E*-polarization, there is no problem arising from charges accumulating on the interface, and the variations of  $\rho_A$  in the region of the interface are much as we would expect for each of the models considered.

The phase variations of the 3 calculated components  $E_x(\phi_{E_x})$ ,  $H_y(\phi_{H_y})$ , and  $H_z(\phi_{H_z})$  across the surface relative to the end point above the lower conducting medium are shown in Figure 5.

In  $\phi_{E_x}$  there is a minimum on the higher conducting side of the surface contact. This minimum moves farther away from the contact and broadens as the period increases. The effects of the shelf and step contacts are strongly evident at 0.003 hz.

The variation of  $\phi_{H_y}$  across the surface of the vertical discontinuity model 1 changes slightly for the 4 frequencies. For the two other models, the change in  $\phi_{H_y}$  as the frequency goes from 0.01 hz to 0.0003 hz is considerable. The shelf and step models show their characteristic differences at all 4 frequencies but most obviously at 0.003 hz and 0.001 hz.

$\phi_{H_z}$  has a minimum on the higher conducting side of the surface contact in all 3 models. This minimum decreases as the period increases. At 0.01 hz, model 3 shows an abrupt step in  $\phi_{H_z}$  over the subsurface corner of the shelf;  $\phi_{H_z}$  for model 2 is much smoother. At 0.003 hz, the shelf corner of model 3 is again marked by a bump, while  $\phi_{H_z}$  for model 2 changes even more smoothly. As the period increases, the effects of the subsurface structures remain but become less prominent.

(Text continued on page 66)

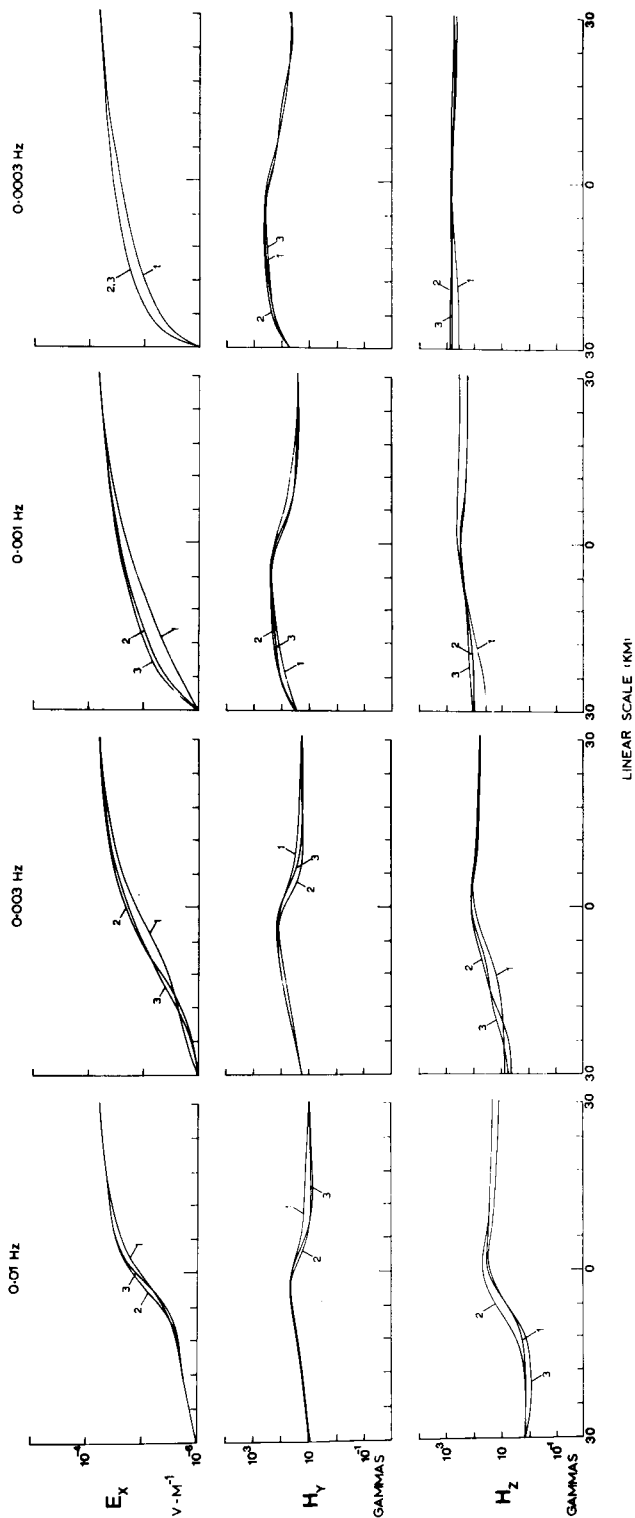


FIG. 3.  $I_z$ -polarization.  $E_x$ ,  $H_y$ , and  $H_z$  for the (1) vertical, (2) step, and (3) shelf models.

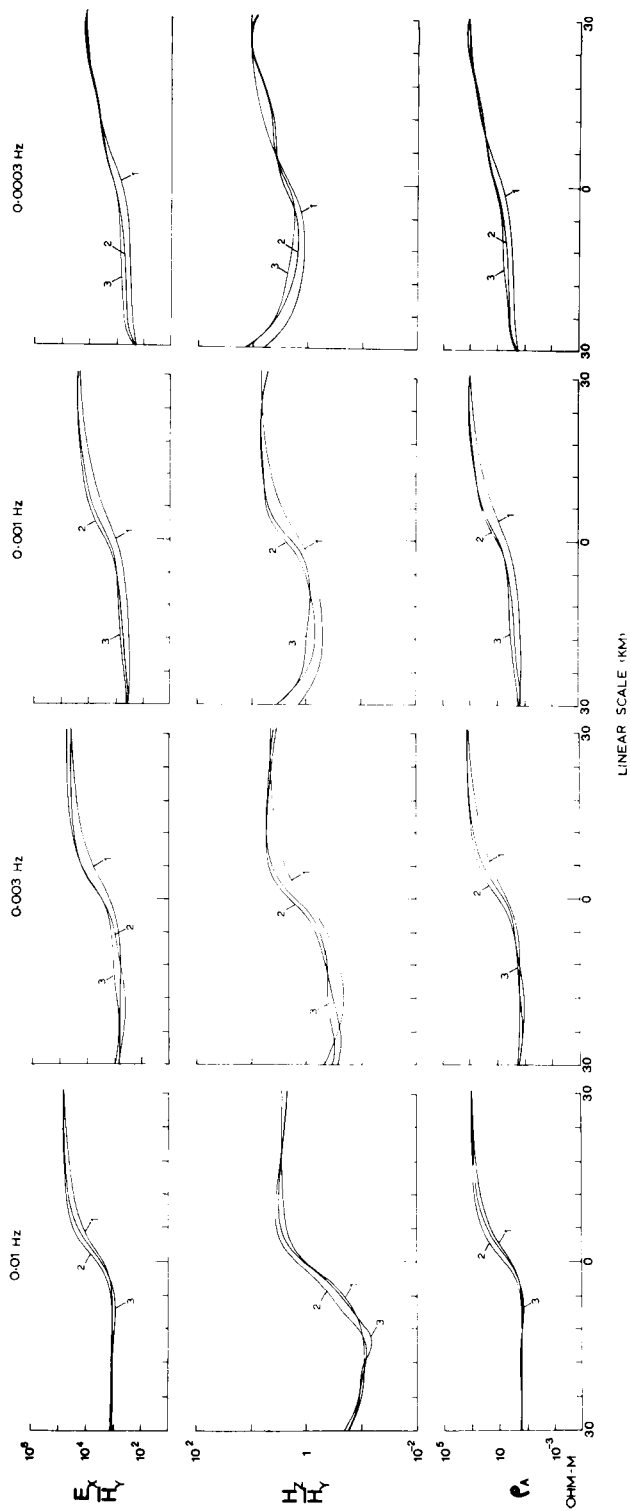


FIG. 4. E-polarization.  $E_x/H_y$ ,  $H_z/H_y$ , and  $\rho_A$  for the (1) vertical, (2) step, and (3) shelf models.

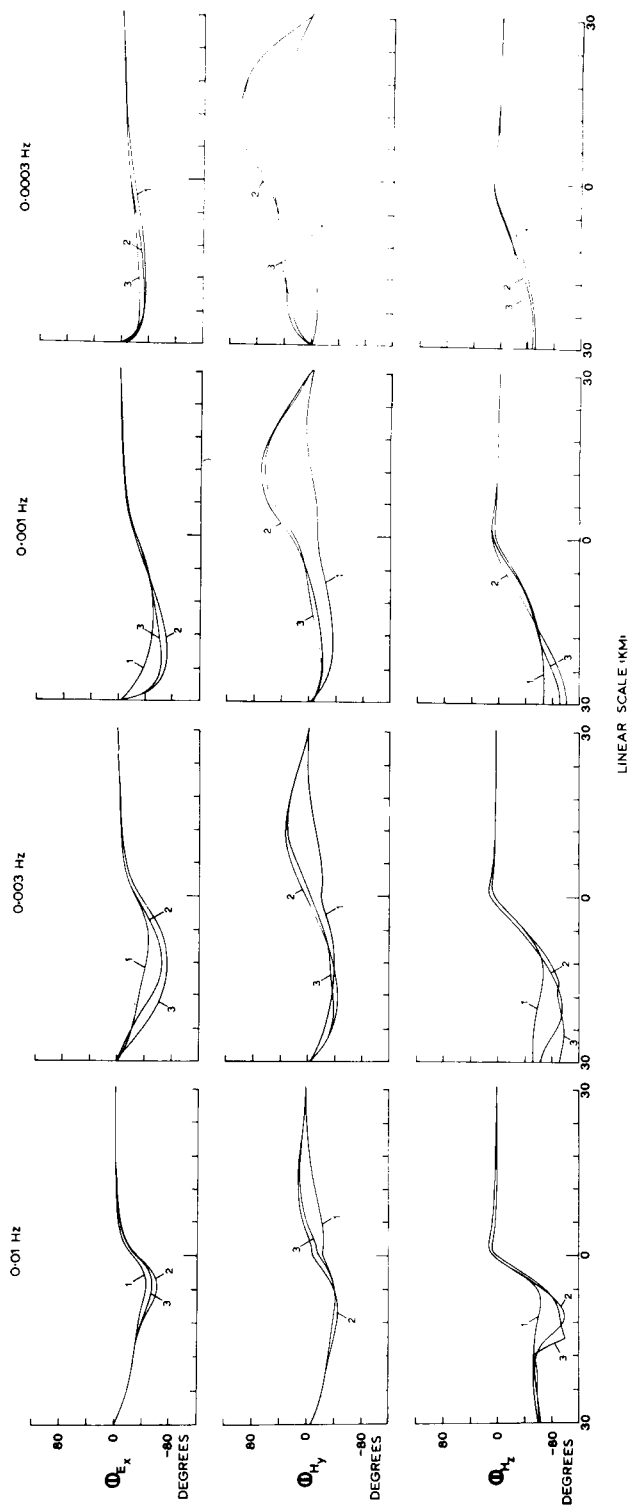


FIG. 5.  $E$ -polarization. The phases of  $E_x(\phi_{E_x})$ ,  $H_y(\phi_{H_y})$ , and  $H_z(\phi_{H_z})$  in degrees across the surfaces of the (1) vertical, (2) step, and (3) shelf models.



## DISCUSSION OF RESULTS

We observe a fundamental difference between the two polarity cases. The apparent resistivity calculated for the  $H$ -polarization case across the contact between the two conductivity regions varies rapidly near the contact and is discontinuous. This is due to a buildup of charge at the interface. Dosso (1966) exhibits a rapidly changing  $E$  component near the edge of his wedge and block model in analog studies of variations near a coastline. The behavior Dosso found is similar to the effect in  $E_y$  obtained here and would lead to a similar variation in the apparent resistivity. For the  $E$ -polarization case,  $E_x$  and the apparent resistivity change continuously near the contacts. The curves for  $E_x$ ,  $H_y$ , and  $H_z$  are similar to those obtained by Dosso for his  $E$ -polarization case.

It is clearly of interest to study the  $H$ -polarization case and variations near lateral inhomogeneities, but for accuracy in interpretation of apparent resistivity values near the interfaces between two media of different conductivity, the  $E$ -polarization case is more suitable. If, in field measurements, the strike of the feature under

investigation can be determined, it is clear that resistivity values calculated from measurements of magnetic field perpendicular to the strike and electric field parallel to the strike will be most directly useful.

## ACKNOWLEDGMENTS

The authors wish to thank the University of Exeter for the use of the university computer and the Computer Department for help and advice. One of us (F. W. J.) wishes to thank the National Research Council of Canada for financial assistance in the form of a postdoctorate fellowship during his stay in England.

## REFERENCES

- Dosso, H. W., 1966, Analogue model measurements for electromagnetic variations near a coastline: *Can. J. Phys.*, v. 3, p. 917.
- Jones, F. W., and Price, A. T., 1969, The perturbation of an alternating field by a conductivity anomaly: *IAGA Bulletin No. 26*, Abstract III-106, p. 196.
- 1970a, The perturbations of alternating geomagnetic fields by conductivity anomalies: *Geophys. J.R.A.S.* v. 20, p. 317.
- 1970b, The geomagnetic effects of two-dimensional conductivity inhomogeneities at different depths: *Geophys. J. Roy. Astr. Soc.*, In press.